Analysis on Energy Efficiency of Large Scale Intelligent Reflecting Surface-Enabled Networks

Youjia Chen, *Member, IEEE*, Baoxian Zhang, Jinsong Hu, *Member, IEEE*
David López-Pérez, *Senior Member, IEEE*, Ming Ding, *Senior Member, IEEE*

***Abstract*—Intelligent reflecting surfaces (IRSs) have been proposed in recent years as a promising technology to enhance signal quality at high frequencies and save energy. In this paper, a Poisson bipolar network model with line segments is used to analyze the energy efficiency (EE) of an IRS-assisted, large-scale network. Specifically, we investigate the performance impact of the IRS configuration, in particular, the number of IRS elements and the phase-shifting resolution of each element. Using customized energy consumption and channel estimation models, we obtain the theoretical trade-off between signal quality and energy consumption as a function of these IRS configurations. The optimal number of elements and phase-shifting resolution of the IRS are also derived. Our results show that IRS technology has great potential for improving the EE of dense networks if their static energy consumption is small enough. Simulation results verify the accuracy of the obtained theoretical results.**

***Index Terms*—Energy efficiency, intelligent reflecting surface, phase-shifting resolution**

I. Introduction

Intelligent reflective surfaces (IRSs), comprised of a large number of reflective elements, are capable of altering the electromagnetic behavior of the radio channel. Explicitly, each IRS element can be independently tuned to change the reflection angle of an incident wave, allowing to reconfigure the wireless environment and focusing the electromagnetic energy on a predesigned direction or a subspace of the channel.

Although an IRS is considered to be an almost passive device, energy consumption is still needed to realise an on-demand adjustment of the configuration of the IRS. It is thus important to understand the energy efficiency of an IRS —and more importantly, of a large-scale network equipped with IRSs— to assess whether this technology can break the increasing energy consumption trend of 5G deployments.

Recently, many works have focused on the analysis of the energy efficiency (EE) of an IRS-assisted wireless link. In [1], the transmission rate and EE of an IRS-assisted channel were compared to that of a channel aided by a classic decode-and-forward relay. It concluded that large-size IRSs can outperform relays in terms of EE. In [2], the EE of an IRS-assisted link was theoretically derived, paying particular attention to the optimal number of elements that an IRS should have. In [3] a multi-cast scenario was considered, and the optimal number of elements in an IRS to maximize EE was investigated. In [4], to maximize the EE of an IRS-assisted MISO link, the BS's transmission power and the IRS's phase configuration were jointly optimized. Similarly, in [5], considering the hardware impairments in such an IRS-assisted MISO link, the BS's transmision power was optimized to maximize the EE. In [6], the overhead for channel estimation and phase configuration related to IRSs were also considered when investigating the transmission rate and EE of an IRS link.

On the other hand, several other works have focused on the performance of an IRS-assisted large-scale network. In [7], the coverage and IRS-association probability were investigated relying on stochastic geometry. In [8], [9], interference scattered by the IRSs in a network was investigated to obtain a practical assessment of the system performance. In [10], the coverage probability and the EE in an IRS-assisted mmWave network were studied, which revealed the performance impact of the density of deployed IRSs. Importantly, it should be noted that the trade-off between network performance and energy consumption due to the number of IRS elements and resolution bits has not been well investigated.

In this paper, we analyze for the first time the EE of an IRS-assisted large-scale network, jointly considering the number of elements in the IRS and their phase resolution as well as the overhead of the IRS's phase control. Importantly, we investigate the concavity of the EE of reflective paths w.r.t. the number of IRS elements and their phase resolutions, and find the optimal solutions.

II. System Model

A. Network deployment model

We consider a Poisson bipolar model, in which the transmitters —the BSs— form a Poisson point process (PPP) Φ_B of intensity λ_b, and each one of them has a dedicated receiver —a dedicated UE—, located at a distance R in a random direction uniformly distributed in $[0, 2\pi)$. The blocking objects are modelled by line-segments of length L, whose centers also form another PPP Φ_O of intensity λ_o. The line-segments have a random orientation that is uniformly distributed in $[0, \pi)$ [1].

Following a given IRS roll-out strategy, we assume that only a fraction of the objects are equipped with IRSs, and

This work was supported by the Natural Science Foundation of Fujian Province under Grant 2022J01081 and Grant 2020J05106, and the National Natural Science Foundation of China under Grant 62271150 and Grant 62001116. Youjia Chen, Baoxian Zhang and Jinsong Hu are with Fujian Key Lab for Intelligent Processing and Wireless Transmission of Media Information, College of Physics and Information Engineering, Fuzhou University, China. E-mail: {youjia.chen, N191127051, jinsong.hu}@fzu.edu.cn. David López-Pérez is with Universitat Politècnica de València. E-mail: dr.david.lopez@ieee.org. Ming Ding is with Data61, CSIRO, Australia. E-mail: ming.ding@data61.csiro.au.

[1]Due to the line-segment model, instead of the rectangle model, the effective range is $[0, \pi)$ but not $[0, 2\pi)$.

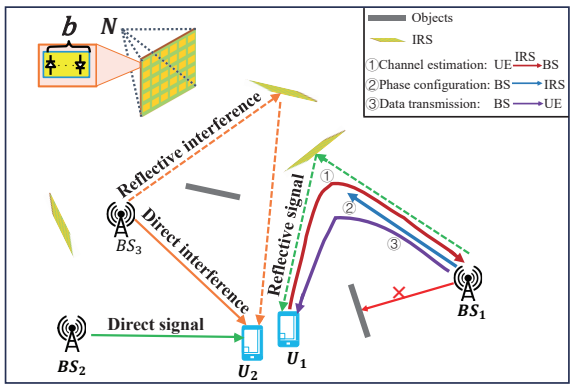

Fig. 1. A Poisson bipolar modeled IRS-aided wireless system.

that if an object is equipped with IRS technology, an IRS is deployed on both sides of the representing line-segment. Thus, the IRS-equipped objects follow a thinned homogeneous PPP $\Phi_R \in \Phi_O$ of intensity $\lambda_r = \rho\lambda_o$, $\rho \in [0,1]$.

As for the IRS, note that each IRS has N elements arranged in a rectangular planar form, and that each one of those IRS elements uses b diodes to control its phase, i.e. b-bit phase resolution. Fig. 1 illustrates the IRS configuration.

Due to the existence of IRSs, both serving and interference signals may arrive at the receiver through a direct or a reflective path, as also illustrated in Fig. 1. From [11], we can derive the probability $\eta(R)$ of a direct path existing between the transmitter and the receiver as $\eta(R) = \exp(-\frac{2\lambda_o L}{\pi}R)$, where λ_o is the object density, and L is the object length.

Since the direct path results in a stronger received signal strength due to its shorter distance, in the considered model, we assume that the typical BS and its associated UE communicate through a reflective path only when the direct path is blocked, i.e. does not exists. A decision and association scheme is assumed to be in place for the BS to decide whether the communication takes place over the direct or the reflective path, and thus tune the IRS [12]. We do not consider the details of this process, only its overhead in time.

B. Channel model

1) Direct Path: As commonly used, the standard single-slope path loss model is adopted for the direct path with a distance R, i.e. $A_0 R^{-\alpha}$, where A_0 and α are the path loss at the unit distance and the path loss exponent, respectively.

Rician fading is considered for direct path. The channel power gain, h_d, due to Rician multi-path (fast) fading is a random variable with a probability density function (PDF) $f_{\mathrm{h_d}}(h_d) = (K+1)\exp(-K-(K+1)h_d)I_0(2\sqrt{K(K+1)h_d})$, where K is the Rician factor, and $I_0(\cdot)$ is the 0-th order modified Bessel function of the first kind.

Hence, given the distance R, the received signal power S_d at the UE through a direct path can be calculated as $S_d = P_t G_m^2 A_0 R^{-\alpha} h_d$, where P_t is the BS transmit power, and G_m is the transmit and receive antenna gain in the BS and the UE. Assuming that both BSs and UEs are equipped with directional antennas, and a perfect beam alignment, G_m equates to the maximum possible antenna (beamforming) gain.

2) Reflective Path: Multiple reflective paths from a BS to a user may exist in a large-scale networks. Consistent with the largest signal strength association criterion mentioned, the shortest reflected path is the one with the smallest path-loss. The PDF of its distance r is given by Eq. (14) in [9] highly depends on the density of IRSs. According to [13], the path loss of the reflective path via an IRS involves two cases, i.e. near- and far-field scenarios:

$$\begin{cases} \zeta(r) = Ar^{-\alpha}, & \text{near-field;} \\ \zeta(r) \approx A'\left(\frac{r}{2}\right)^{-2\alpha}, & \text{far-field.} \end{cases} \tag{1}$$

The boundary between the near and far field depends both on the signal frequency and the aperture size.

As for the reflected path, the power of its channel gain due to fast fading, h_r, follows a scaled non-central chi-square distribution with degree one [9], i.e. with a PDF $f_{\mathrm{h_r}}(h_r) = \frac{1}{2\sigma^2}\exp\left(-\frac{h_r+\mu^2}{2\sigma^2}\right)\left(\frac{h_r}{\mu^2}\right)^{-\frac{1}{4}} I_{-\frac{1}{2}}\left(\frac{\mu}{\sigma^2}\sqrt{h_r}\right)$, where $I_\nu(\cdot)$ is the first kind modified Bessel function, $\mu = N\frac{\pi}{4(K+1)}\left(L_{\frac{1}{2}}(-K)\right)^2$, $L_{\frac{1}{2}}(\cdot)$ are the Laguerre polynomials of degree $1/2$ and $\sigma^2 = N - N\frac{\pi^2}{16(K+1)^2}\left(L_{\frac{1}{2}}(-K)\right)^4$.

The received signal power S_r via the IRS can be given as $S_r \approx P_t G_m^2 \cdot G_{\mathrm{IRS}}(N) \cdot \epsilon(b) \cdot \zeta(r) h_r$. Expect the antenna gain in the BS and the UE, here $G_{\mathrm{IRS}}(N)$ represents the gain of the IRS due to the number N of IRS elements [14]. And $\epsilon(b)$ represents the IRS's reflection efficiency, which depends on the phase resolution b of the IRS element. According to [15], Fig. 6, $\epsilon(b)$ is concave function.

C. Channel estimation procedures

For direct paths, pilot tone transmissions are needed to estimate the channel from the UE to the BS. We denote by T_E^d the duration of the channel estimation phase.

For the reflective paths, not only such channel estimation is required, but also the configuration of the phase shifts at the IRS. In more details, as shown in Fig. 1, after the UE has sent the pilot tones to the BS for channel estimation purposes, the BS has to calculate and send the optimized phase matrix to the IRS, for it to configure each IRS element's phase before the data transmission[2]. Correspondingly, we denote by T_E^r the duration of the channel estimation, and T_F the duration of such IRS phase configuration.

Embracing the basic channel estimation procedure in [6], with N elements in each IRS, the UE sends N pilot tone sequentially, one after the other, through the IRS to the BS to facilitate channel estimation. Thus we formulate the duration of channel estimation phase as

$$T_E^r(N) = T_0 \times (N+1), \tag{2}$$

where the extra pilot tone is required for the BS to estimate the feedback channel, and T_0 is the time duration of a pilot tone transmission. Note that, alternative and more efficient channel estimation approaches, such as that in [16], may reduce the cost and improve the performance of the system.

[2]Note that the BS also has to estimate the channel between the BS and the IRS, prior to sending such an optimised phase matrix to the IRS.

Besides, T_F depends on the number of IRS elements, phase resolution b, bandwidth of the feedback channel B_F, i.e.

$$T_F(N,b) \approx \frac{Nb}{B_F \log_2(1+\gamma_0)} \tag{3}$$

where γ_0 is signal to interference plus noise ratio (SINR) needed to operate modulation and coding scheme (MCS) used.

III. Derivation of network energy efficiency

A. SINRs for direct and reflective paths

Without loss of generality, we assume that the typical user locates at the origin. The aggregated interference via direct paths comes from the visible BSs for the typical user $\tilde{\Phi}_B$[3], except the typical BS $\mathbf{x}_0$, can be calculated as $I_d = \sum_{\mathbf{x}\in\tilde{\Phi}_B\setminus\mathbf{x}_0} P_t G^d_{\mathbf{x}} A_0 x^{-\alpha} h_{d,\mathbf{x}}$, where $\mathbf{x}$ is the location of the interfering BS, and $x = \|\mathbf{x}\|$ is the corresponding distance to the typical UE, $G^d_{\mathbf{x}}$ is the antenna gain from the interfering BS, which follows the PDF in [14, Eq. (18)], and $h_{d,\mathbf{x}}$ denotes the channel power gain due to multi-path (fast) fading.

The aggregated interference from the reflective paths via the IRSs is complicated to exactly model. Following [9], we model the IRSs as additional interfering sources, which reflect the EM wave out with an equivalent power $\tilde{P}_{\text{IRS}}$:

$$\tilde{P}_{\text{IRS}} = \frac{Q}{2} \times \mathbb{E}_{\tilde{\Phi}'_B, h_d}\left[\sum_{\mathbf{x}'\in\tilde{\Phi}'_B}\left(\sum_{i=1}^{N} P_t G^r_{\mathbf{x}'} A_0 h_{d,\mathbf{x}'} ||\mathbf{x}'-\mathbf{y}_0||^{-\alpha}\right)\right] \tag{4}$$

where Q is the probability that the interfering signal is reflected out by the IRS, calculated by [9, Eq. (23)], and $\frac{1}{2}$ is the probability that the typical BS and its associated UE are located at the same side as the IRS. Note that $\tilde{\Phi}'_B$ denotes the visible BSs to a typical IRS located at $\mathbf{y}_0$, and $G^r_{\mathbf{x}'}$ is the antenna gain between the interfering transmitter and the IRS.

Then, the aggregated interference from the IRSs to the typical UE can be formulated as $I_r = \sum_{\mathbf{y}\in\tilde{\Phi}_R} \tilde{P}_{\text{IRS}} G^r_{\mathbf{y}} A_0 y^{-\alpha} h_{d,\mathbf{y}}$, where $\tilde{\Phi}_R$ is the set of visible IRSs, and $y = \|\mathbf{y}\|$ is the distance between the typical UE to the IRS located at $\mathbf{y}$.

Depending on whether the UE receives information from the direct or reflective path, we have the SINR formulations:

$$\begin{cases} \Gamma_d(R) = \frac{P_t G_m^2 A_0 R^{-\alpha} h_d}{I_d + I_r + N_0}, & \text{with prob. } \eta(R); \\ \Gamma_r(r) \approx \frac{P_t G_m^2 G_{\text{IRS}}(N)\epsilon(b) h_r \cdot \zeta(r)}{I_d + I_r + N_0}, & \text{with prob. 1-}\eta(R). \end{cases} \tag{5}$$

where N_0 is noise power.

B. Transmission rate

Denoting by T the overall duration of the time slot including channel estimation, phase configuration, and data transmission, the achievable UE rate with the ideal MCS via the direct path, R_d, can be formulated from the Shannon theorem as

$$R_d = (1 - \frac{T_E^d}{T}) B \log_2\left(1 + \Gamma_d(R)\right), \tag{6}$$

since a fraction of time $\frac{T_E^d}{T}$ is dedicated to channel estimation. While the achievable UE rate R_r via the reflective path is:

$$R_r = \left(1 - \frac{T_E^r + T_F}{T}\right) B \log_2\left(1 + \Gamma_r(r)\right), \tag{7}$$

since both the channel estimation time T_E^r and the phase configuration time T_F have to be considered.

C. Power consumption and energy efficiency

Similarly to the UE rates R_d and R_r, we formulate the power consumption P^d_{link} and P^r_{link} for direct and reflective transmissions, respectively, as

$$\begin{cases} P^d_{link} = \frac{T_E^d}{T} P_u + (1 - \frac{T_E^d}{T}) P_t, \\ P^r_{link} = \frac{T_E^r}{T} P_u + \frac{T_F}{T} P_t + NbP_0 + \frac{T - T_E^r - T_F}{T} P_t, \end{cases} \tag{8}$$

where P_u is the UE transmit power used for pilot tone transmission, P_t is the BS transmit power used during both the phase configuration and the data transmission, and P_0 is the power consumed per bit of resolution by each phase shifter in each IRS element following prototypes using an diode for one bit phase control.

Denoting by P_{BS} and P_{IRS} the static power consumption of a BS and an IRS when they are idle, i.e. do not transmit/receive or perform phase shifting, respectively, the energy efficiency of the network can be formulated as:

$$\text{EE}_{\text{net}} = \frac{\lambda_b \left[\eta R_d + (1-\eta) R_r\right]}{\lambda_b \left[\eta P^d_{link} + (1-\eta) P^r_{link}\right] + \lambda_b P_{\text{BS}} + \rho \lambda_o P_{\text{IRS}}}. \tag{9}$$

Note that we assume that the network is fully loaded.

IV. Impact of IRSs on energy efficiency

In this section, we analyze the impact of the number N of IRS elements and their phase resolution b on energy efficiency.

To facilitate the analysis and draw conclusions, we take the liberty of isolating energy efficiency of reflective links, i.e.

$$\text{EE}_r = \frac{(1-\eta)\lambda_b \left(1 - \frac{T_E^r + T_F}{T}\right) B \log_2\left(1 + \Gamma_r(r)\right)}{(1-\eta)\lambda_b \left[\frac{T_E^r}{T} P_u + (1 - \frac{T_E^r}{T}) P_t + NbP_0\right] + \lambda_b P_{\text{BS}} + \rho \lambda_o P_{\text{IRS}}}. \tag{10}$$

1) Effect of the phase resolution: To investigate the impact of the phase resolution b on EE_r, assuming a continuous b for simplicity, we have

Lemma 1. *When* $\frac{[\frac{T_E^r}{T} P_u + (1 - \frac{T_E^r}{T}) P_t] + \frac{1}{1-\eta} P_{BS} + \frac{1}{(1-\eta)\lambda_b} \rho \lambda_o P_{IRS}}{P_0} > (T - T_E^r) B_F \log_2(1 + \gamma_0)$*, the energy efficiency* EE_r *is concave w.r.t. the phase resolution* b *in its feasible region* $0 < b < \frac{(T - T_E^r) B_F \log_2(1+\gamma_0)}{N}$.

Proof. See Appendix A.

Taking advantage of the concavity of the EE_r, a standard bisection or gradient descent method can be adopted to find the optimal phase solution for the following optimization problem:

$$\begin{aligned} \underset{b}{\text{maximize}} \quad & \text{EE}_\text{r} \\ \text{s.t.} \quad & 0 < b < \frac{(T - T_E) B_F \log_2(1+\gamma_0)}{N} \end{aligned} \tag{11}$$

Then we round the optimal solution to the nearest integer to obtain a practical solution b^*.

[3] $\tilde{\Phi}_B$ follows a non-stationary PPP with a density $\exp(-\eta(R)x)\lambda_b$ [9].

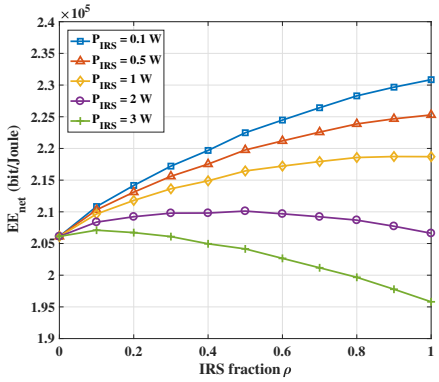

Fig. 2. EE_{net} with various P_{IRS} in far-field scenario.

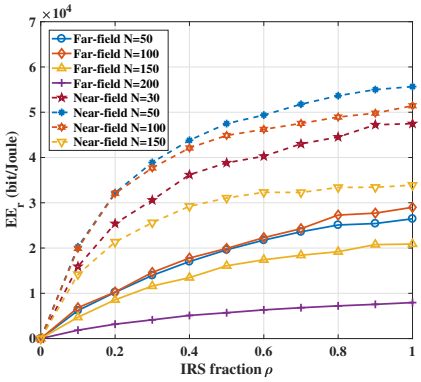

Fig. 3. EE_{r} with different element numbers N.

2) Effect of the number of IRS elements: For the effect of the number N of IRS elements on EE_{r}, assuming a continuous N for simplicity, we have

Lemma 2. *When* $P_t + \frac{1}{1-\eta}P_{BS} + \frac{\rho\lambda_o}{(1-\eta)\lambda_b}P_{IRS} \gg bP_0 + (P_u - P_t)\frac{T_0}{T}$, $EE_r(N)$ *is concave w.r.t.* N.

Proof. See Appendix B.

Similarly a standard gradient descent method and rounding process can be adopted to find the optimal number of IRS elements N^* for the following optimization problem:

$$\begin{aligned} \underset{N}{\text{maximize}} \quad & \text{EE}_{\text{r}} \\ \text{s.t.} \quad & 0 < N < \frac{T-T_0}{T_0+b/B_F\log_2(1+\gamma_0)} \end{aligned} \tag{12}$$

Furthermore, the joint optimization of b and N can be performed also by iteratively solving (17) and (18).

V. Simulation Results and Discussion

In this section, we present simulation results on the energy efficiency of an IRS-assisted, large-scale, bipolar network, and discuss the performance impact of the IRS parameters. The density of transmitters and objects are set to $\lambda_b = 80\,\text{units/km}^2$ and $\lambda_o = 800\,\text{units/km}^2$, respectively. The object length is assumed as $L = 25\,\text{m}$. Unless otherwise stated, the BS transmit power used during the data and control feedback phases is set to P_t=30 dBm, while their bandwidths to B = 5 MHz and B_F =2 MHz, respectively. Besides, the static power consumption values of the BS and the IRS are set to $P_{\text{BS}} = 160\,W$ and $P_{\text{IRS}} = 1\,W$, respectively, while the power consumption per bit of resolution of an IRS element to $P_0 = 3\,\text{dBm}$. The UE transmit power used for pilot tone transmission is assumed to be $P_u = 23\,\text{dBm}$ [4].

We investigate both near- and far-field scenarios[4]: 1) In the far-field scenario, λ_b = 80 units/km^2, and the distance between the transmitter and the receiver is set to $R = 50$ m. 2) In the near field scenario, λ_b = 100 units/km^2 and $R = 25$ m. Note that the direct path in this case is assumed to be blocked.

[4]The boundary of the far-field and the near-field depends both on the frequency and the aperture size. For instance, at 30GHz and with an IRS length of 0.5m, the boundary is around 50m.

Fig. 2 shows the network energy efficiency EE_{net} versus the IRS fraction ρ for various static IRS power consumption P_{IRS} in the far-field scenario. Intuitively, EE_{net} decreases with the increase of P_{IRS}. Moreover, our results show that, when the static IRS power consumption P_{IRS} is small, e.g. 0.1 and 0.5 W, the network energy efficiency EE_{net} increases with the growth of the IRS fraction ρ. This indicates that, due to the small P_{IRS}, the increase in the reflective signal power resulting from the deployment of more IRSs outweighs that of the static energy consumption. In contrast, when P_{IRS} is large, deploying more IRSs leads to a decrease of EE_{net} with the increase of ρ, as the IRS energy consumption becomes more relevant. From these results, it can be concluded that the static IRS power consumption P_{IRS} plays a crucial role in the rollout and sustainability of IRS-assisted, large-scale networks. It also implies that almost passive IRSs with a small static IRS power consumption are key to the success of this technology.

Fig. 3 shows the energy efficiency of the reflective links EE_{r} versus the IRS fraction ρ for various numbers N of IRS elements. The assumed phase resolution is $b = 1$. The dashed and solid lines present EE_{r} in the near- and far-field scenarios, respectively. The results indicate that the energy efficiency of the reflective links EE_{r} generally increases with the IRS fraction ρ in both scenarios, as more IRSs enhance the reflective signal power. The increasing trend is more obvious when the number N of IRS elements is small, as the addition of a few IRSs addresses large coverage holes. Most importantly, consistent with the theoretical conclusion in **Lemma 1**, we can see that, given an IRS fraction ρ, EE_{r} first increases with N, and after some point, it decreases with it. Note that in the far-field scenario, $N = 100$ achieves the best performance, while in the near-field scenario, $N = 50$ is the best setting. The main reason behind this non-linear behaviour is the trade-off mentioned earlier between signal strength and power consumption resulting from the deployment of more IRS elements. Note that increasing N quickly becomes detrimental in the near-field scenario as the signal propagates better as a result of the smaller path losses, and adding more IRSs only introduces interference.

Fig 4 shows the impact of the phase resolution b on the energy efficiency of the reflective links EE_{r}. The trend with the phase resolution b is similar to that with the number N

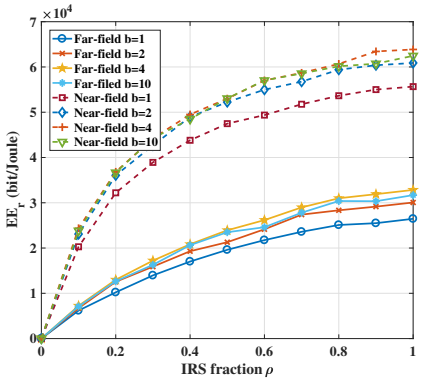

Fig. 4. $\mathrm{EE_r}$ with various phase resolution b.

of IRS elements, i.e. it first increases with the increase of b, when b is small, and then decreases with it, when b further increases. This phenomenon corroborates the theoretical result in **Lemma 2**. When the phase resolution b increases from 1 to 4, there is a noticeable improvement in the energy efficiency of the reflective links $\mathrm{EE_r}$, as the reflection efficiency ϵ of the IRS increases from 0.4 to 0.92, thus increasing the received signal strength through the reflective path, When the resolution level increases to 10, however, meaning that there are 10 diodes behind each IRS element, $\mathrm{EE_r}$ decreases due to the corresponding increase in IRS power consumption and the time T_F invested in the phase configuration. Similar to Fig. 3, we can also see that the near- and far-field scenarios follow the same trends, with the near-field case having a larger $\mathrm{EE_r}$.

VI. Conclusion

In this paper, the network energy efficiency of an IRS-assisted, large-scale network has been analysed. Our results show the trade-off between the network performance and the energy consumption, and indicate that it is unfeasible to continuously increase the network energy efficiency by simply increasing the number of IRS elements and diodes behind them. Nearly passive IRS elements are necessary to make IRS-assisted networks sustainable.

Appendix A
Proof of **Lemma 1**

$\mathrm{EE_r}$ can be simplified as: $\mathrm{EE_r}(b) = f(b)\cdot g(b)$, where $f(b) \triangleq \frac{C_1 - C_2 b}{C_3 + C_4 b}$ and $g(b) \triangleq B\log_2(1+C_5\varepsilon(b))$. Also, $C_1 = 1 - \frac{T_E^r}{T} > 0$, $C_2 = \frac{N}{TB_F\log_2(1+\gamma_0)} > 0$, $C_3 = \frac{T_E^r}{T}P_u + (1-\frac{T_E^r}{T})P_t + \frac{1}{1-\eta}P_{BS} + \frac{\rho\lambda_o}{(1-\eta)\lambda_b}P_{\mathrm{IRS}} > 0$, $C_4 = NP_0 > 0$, and $C_5 = \frac{P_t G_m^2 G_{\mathrm{IRS}} A_0^2 h_r \zeta}{I_d + I_r + N_0} > 0$. Within the feasible region $b \in (0, \frac{C_1}{C_2})$, we have $f(b) > 0$ and $f^{'}(b) < 0$; $g(b) > 0$ and is a concave function; $\frac{\partial \mathrm{EE_r}}{\partial b}\mid_{b=0} > 0$ and $\frac{\partial \mathrm{EE_r}}{\partial b}\mid_{b=\frac{C_1}{C_2}} < 0$.

For the equation $\frac{\partial \mathrm{EE_r}}{\partial b} = 0$, i.e. $\frac{f(b)}{f^{'}(b)} = -\frac{g(b)}{g^{'}(b)}$. Given $\frac{f(b)}{f^{'}(b)}$ is a quadratic function, and $\frac{f(b)}{f^{'}(b)}\mid_{b=0} < 0$ and $\frac{f(b)}{f^{'}(b)}\mid_{b=\frac{C_1}{C_2}} = 0$. While $-\frac{g(b)}{g^{'}(b)}$ is monotonically decreasing from $-\frac{g(b)}{g^{'}(b)}\mid_{b=0} = 0$. When the axis of symmetry of $\frac{f(b)}{f^{'}(b)}$ is smaller than 0, in the feasible region, it is monotonically increasing. Since $-\frac{g(b)}{g^{'}(b)}$ is monotonically decreasing, they have only one intersection.

Appendix B
Proof of **Lemma 2**

$\mathrm{EE_r}$ can be simplified: $\mathrm{EE_r}(N) = \frac{1-D_2 N}{D_3 + D_4 N}\cdot B\log_2(1 + D_5 G_{\mathrm{IRS}}(N))$, where $D_2 = \frac{T_0}{T} + \frac{b}{TB_F\log_2(1+\gamma_0)} > 0$, $D_3 = P_t + \frac{1}{1-\eta}P_{BS} + \frac{\rho\lambda_o}{(1-\eta)\lambda_b}P_{\mathrm{IRS}} > 0$, $D_4 = bP_0 + (P_u - P_t)\frac{T_0}{T}$, and $D_5 = \frac{P_t G_m^2 \epsilon(b) A_0^2 h_r \zeta}{I_d + I_r + BN_0} > 0$. Considering the extremely large power disparity P_0 and P_{BS}, $\eta < 1$ and $P_u < P_t$, we have $D_3 \gg D_4$, and the approximation $\mathrm{EE_r}(N) \approx q(N)\cdot k(N)$, where $q(N) \triangleq \frac{D_1 - D_2 N}{D_3}$ and $k(N) \triangleq B\log_2(1 + C_5 G_{\mathrm{IRS}}(N))$.

Within the feasible region $N \in (0, \frac{1}{D_2})$, we have $q(N)$ is linearly decreasing function, from 1 to 0; $k(N) > 0$ and increases with N. For the equation $\frac{\partial \mathrm{EE_r}}{\partial N} = 0$, i.e. $\frac{q(N)}{q^{'}(N)} = -\frac{k(N)}{k^{'}(N)}$. We have $\frac{q(N)}{q^{'}(N)}$ is monotonically increasing from 0 to $\frac{2}{D_2}$. While $-\frac{k(N)}{k^{'}(N)}$ is a monotonically decreasing function since $k(N)$ is concave [14]. Hence, the number of their intersection is one.

References

[1] E. Björnson, O. Özdogan, and E. G. Larsson, "Intelligent reflecting surface versus decode-and-forward: How large surfaces are needed to beat relaying?" *IEEE Commun. Lett.*, Feb. 2020.

[2] A. Zappone, M. Di Renzo, X. Xi, and M. Debbah, "On the optimal number of reflecting elements for reconfigurable intelligent surfaces," *IEEE Wireless Commun. Lett.*, Mar. 2021.

[3] L. Du, W. Zhang, J. Ma, and Y. Tang, "Reconfigurable intelligent surfaces for energy efficiency in multicast transmissions," *IEEE Trans. Veh. Technol.*, Jun. 2021.

[4] C. Huang, A. Zappone, G. C. Alexandropoulos, M. Debbah, and C. Yuen, "Reconfigurable intelligent surfaces for energy efficiency in wireless communication," *IEEE Trans. Wireless Commun.*, vol. 18, no. 99, pp. 4157–4170, Aug. 2019.

[5] S. Zhou, W. Xu, K. Wang, M. Di Renzo, and M.-S. Alouini, "Spectral and energy efficiency of IRS-assisted MISO communication with hardware impairments," *IEEE Wireless Commun. Lett.*, Sep. 2020.

[6] A. Zappone, M. Di Renzo, F. Shams, X. Qian, and M. Debbah, "Overhead-aware design of reconfigurable intelligent surfaces in smart radio environments," *IEEE Trans. Wireless Commun.*, Jan. 2021.

[7] M. A. Kishk and M.-S. Alouini, "Exploiting randomly located blockages for large-scale deployment of intelligent surfaces," *IEEE J. Sel. Areas Commun.*, Apr. 2021.

[8] Y. Zhu, G. Zheng, and K.-K. Wong, "Stochastic geometry analysis of large intelligent surface-assisted millimeter wave networks," *IEEE J. Sel. Areas Commun.*, vol. 38, no. 8, pp. 1749–1762, Aug. 2020.

[9] Y. Chen, B. Zhang, M. Ding, D. López-Pérez, M. Hassan, M. Debbah, and Z. D. Chen, "Downlink performance analysis of intelligent reflecting surface-enabled networks," *IEEE Trans. Veh. Technol.*, vol. 72, no. 2, pp. 2082–2097, Feb. 2023.

[10] L. Yang, X. Li, S. Jin, M. Matthaiou, and F.-C. Zheng, "Fine-grained analysis of reconfigurable intelligent surface-assisted mmwave networks," *IEEE Trans. Commun.*, vol. 70, no. 9, pp. 6277–6294, Sep. 2022.

[11] T. Bai, R. Vaze, and R. W. Heath, "Using random shape theory to model blockage in random cellular networks," in *2012 SPCOM*, Jul. 2012, pp. 1–5.

[12] L. You, J. Xiong, D. W. K. Ng, C. Yuen, W. Wang, and X. Gao, "Energy efficiency and spectral efficiency tradeoff in RIS-aided multiuser MIMO uplink transmission," *IEEE Trans. Signal Process.*, vol. 69, pp. 1407–1421, Dec. 2021.

[13] M. Di Renzo, F. Habibi Danufane, X. Xi, J. de Rosny, and S. Tretyakov, "Analytical modeling of the path-loss for reconfigurable intelligent surfaces ¨c anomalous mirror or scatterer?" in *2020 IEEE SPAWC*, May 2020, pp. 1–5.

[14] O. Özdogan, E. Björnson, and E. G. Larsson, "Intelligent Reflecting Surfaces: Physics, Propagation, and Pathloss Modeling," *IEEE Wireless Commun. Lett.*, vol. 9, no. 5, pp. 581–585, May 2020.

[15] D. Headland, Y. Monnai, D. Abbott, C. Fumeaux, and W. Withayachumnankul, "Tutorial: Terahertz beamforming, from concepts to realizations," *APL Photonics*, vol. 3, no. 5, p. 051101, Feb. 2018.

[16] H. Guo and V. K. N. Lau, "Uplink cascaded channel estimation for intelligent reflecting surface assisted multiuser MISO systems," *IEEE Trans. Signal Process.*, vol. 70, pp. 3964–3977, Jul. 2022.